

A machine learning-based approach towards the improvement of SNR of pulsar signals

Amitesh Singh ¹ , Kamlesh N Pathak ¹

¹ Sardar Vallabhbhai National Institute of Technology, Surat, India-395007; u17me100@med.svnit.ac.in

Version April 27, 2022 submitted to Journal Not Specified

Abstract: Many pulsar folding algorithms are currently deployed to generate strong SNRs for the total intensity profiles. But they require large observation times to improve the SNR effectively. New approaches to de-noise the pulsar total intensity data have sprung up over the years, powered by Machine learning and Deep learning algorithms. In the current work, efforts are made to implement the currently proposed supervised machine learning models, such as ensembling techniques like Decision Tree Regressor, Random Forest Regressor, Adaboost Regressor, Gradient Boosting Regressor (GBR), K-Nearest Neighbours(KNN), and Support Vector Regressor (SVR) to find out the best possible algorithm which can work over a variety of pulsars from the EPN database of pulsars. All the data used in this work is extracted from the European Pulsar Network (EPN) database of pulsar profiles. The training dataset is obtained by post-processing the pulsar profile data from the EPN database and testing is performed on a preselected portion of the original data. The results are obtained by testing the above algorithms for 10 different pulsars, including some historically significant ones, and the predicted profiles are plotted. We find that Gradient boosting regressor works the best in denoising pulsar data, followed closely by KNN regressor. This work also emphasizes that there is a reduction in the number of periods of folding by 35-40% when a combination of machine learning models with the existing pulsar folding techniques like Fast Folding Algorithm(FFA) is employed, which in turn can further reduce the pulsar observation times for the telescopes hunting for pulsars today.

Keywords: dedispersion; SNR; DM(dispersion measure); Machine Learning; Fast Folding Algorithm; Pulsar total intensity profiles; the EPN database of pulsars

1. Introduction

Pulsars are extremely fast rotating neutron stars that emit pulses of electromagnetic radiation at very regular intervals.[1]. For those high energy and extreme physics which cannot be emulated on earth, pulsars are the right kind of laboratories to test many of our theories. We have detected more than 2700 different pulsars as of today. Many telescopes such as Parkes Radio Telescope[2] [3], Giant Meter Wave Telescope (GMRT)[4], Fermi Gamma-Ray Space Telescope [5] and others have been looking for different classes of pulsars for a relatively long time now. Unfortunately, almost all the pulsar signals observed by the telescopes worldwide are digital signals marred by several possible noise sources. A standard form of telescope data can be represented as:-

$$O(t) = S(t) + N(t) + G(t) + c \quad (1)$$

where $O(t)$ represents the observed data with respect to time, $S(t)$ represents the embedded pulsar signal, $N(t)$ represents the cumulative noise from different sources, $G(t)$ contains the various glitches, and c is the DC Offset.

To extract the signals from the noise, digital signal processing becomes a vital tool. Many different tools are available to process the pulsar data, such as PSRCHIVE [6], DSPSR [7], HIPSR [8], pinta[9] and others. These are employed for a variety of purposes such as dedispersion, pulsar folding, lightcurve extraction and many more features.

One of the major problems faced today in the identification of pulsars is the very low SNR of the raw signals (SNR 1-5). Before we can study the shape and size of the pulse emitted by pulsars clearly; we need to first increase the signal to noise ratio (SNR) of the observed signals embedded in noise. Primarily, after the pulsar signal is dedispersed, we generally employ pulsar folding techniques to boost the SNR of the pulsar, but it gets increasingly more computationally intensive as the number of periods of folding increase. We reach acceptable SNRs only after a lot of folding periods, which forces the telescopes to record data for large observation times. To solve this particular problem, we propose the application of machine learning algorithms that can supplement the pulsar folding techniques in improving the pulsar SNR so that the observation times of a telescope are significantly reduced.

Machine Learning is a fast-growing field, and it has been utilized to solve a multitude of problems in Pulsar Astronomy over the recent years. Recent advances in ML algorithms have enabled us to classify pulsars. In [10], a new, two-stage approach for identifying and classifying dispersed pulse groups (DPGs) in single-pulse search output is presented, and [11] has reduced the number of pulsar candidates to be visually inspected by several orders of magnitude. In [12], a strategy to classify a big set of unbalanced pulsar data has been proposed, and [13] works on improving the SNR of a pulsar candidate through recurrent neural networks (RNN). SNR of a pulsar is the most important feature for denoising them using Machine learning as demonstrated in [14]. Recent studies like [15] and [16] present a holistic review of machine learning-based pulsar search algorithms.

[13] has focused on a similar problem while working on the Vela pulsar data from the RXTE mission, where they have proposed a different (deep learning-based) approach to boost the SNR of pulsars. Our work improves upon the foundation laid down by them as we obtain higher output SNRs for denoised profiles, which would help us study these pulsars efficiently and extract the pulse shape information. Deep learning requires high end processing, including large RAMs, strong GPUs and powerful CPUs. Machine learning models are computationally less expensive, and can be employed using much lower processing power. This fact has primarily motivated this work. We obtain more efficient SNR improvement with much lower MSE values than the above-cited paper.

This work will pave the way for a robust machine learning algorithm which can work in tandem with pulsar folding techniques to give us faster signal extraction times and lower telescope observation times. We aim to reduce the noise from different pulsars and improve the SNR of the time-series data containing the total pulsar intensities. We have tested many state of the art machine learning approaches to solve the problem of low SNRs of the pulsar signals. In this work, we have used 10 pulsars available at the EPN database, an open-access database put forward by many generous contributors [17].

2. Dataset Preparation

We have used the pulsar single pulse data from the EPN database of pulsars [18] [19]. The details of the pulsars used and their properties are listed below and the values of the pulsar period and dispersion measures are derived from the ANTF Pulsar Catalogue [20]. Several significant pulsars have also been tested, for example, J1748-2446ad for being the fastest spinning Neutron star pulsar [21], J1300+1240 for being the pulsar around which the first extrasolar planets were discovered [22], J1915+1606 for being the

first detected pulsar in a binary system[23], J0738-4042 for being the first pulsar signal ever to have been affected by asteroids[24], and J0250+5854 for being the pulsar with the longest detected period[25]. :- :-

Table 1

Pulsar	Period (s)	DM (pc/cm^3)	Sampling frequency (MHz)
J0006+1834	0.694	11.410	430
J0152-1637	0.833	11.925	408
J0437-4715	0.00575	2.645	436
J1829-1751	0.307	217.108	1408
J2053-7200	0.341	17.300	660
J2145-0750	0.0160	8.997	1510
J1300+1240	0.00622	10.165	1410
J1915+1606	0.0590	168.77	1560
J1921+2153	1.337	12.443	1418
J0738-4042	0.375	160.896	1375

2.1. Data preprocessing

Single-pulse data does not have enough data points to train the model efficiently. Generally, more the number of input data points, more accurate is the model training. The performance accuracy maximizes at a particular input data size and then decreases due to overfitting. To provide the models with enough data points to work with, we have converted the single pulse signal data into hundreds of pulses. The exact number depends upon the sampling rate of pulsar data from the EPN database. At this stage, signals are relatively pure.

2.2. Gaussian Noise injection

Once we have data of multiple pulses, we inject Gaussian noise to the signals with a mean of 0 and a standard deviation of 0.2, so that the raw signals have an SNR hovering around 4, to mimic the low SNRs observed in the raw data from the telescopes. The present work focuses exclusively on improving the SNR, reducing pulsar folding periods and decreasing signal processing time. A complete pipeline for the data generation process is given below:-

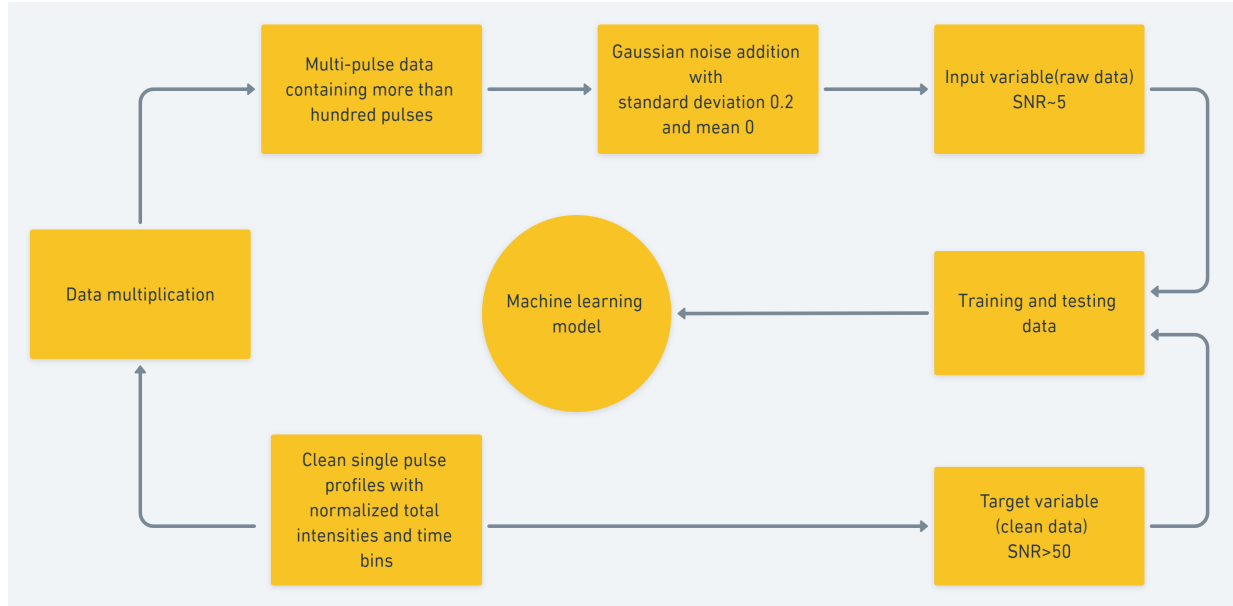


Figure 1. A complete data generation pipeline showing the details of all the operations to generate the input and output data

The whole data of a pulsar is divided into training and testing data.

2.3. Training Data

Training data is that data used to make the model learn the various parameters and features of the data we are concerned with. It constitutes a major chunk of all the data, comprising about 70-85%. In our case, training data is a 2D array consisting of 50000 rows and 2 columns, X_{train} and y_{train} , so the training array's shape is (50000,2). Most of the pulsars had a sufficient number of the pulses embedded into the training dataset (more than 100 pulses). Further increasing the training dataset did not show any signs of improvement in the model performance. Thus it resulted in overfitting of the data, which is a phenomenon where the model learns the training data 'too well' but fails to perform on new and unseen testing data [26]. We provide the models with both the values of X_{train} (containing raw data with noisy pulses) and y_{train} (containing the denoised profiles) during training. The training dataset consists of 83.33% of the total dataset of a pulsar in all the pulsars we have tested and for all the algorithms used to compare the relative performances of different models easier.

2.4. Testing Data

Once any machine learning model is trained with the training dataset, it is evaluated on an unseen dataset called 'Testing dataset' to gauge how well the model can predict the outputs for unseen input variables. Testing data comprises 15-30% of the total data. In our case, the testing data is a 2D array consisting of 10000 rows and 2 columns, X_{test} and y_{test} , and so the shape of the testing dataset is (10000,2). Increasing the length of testing data did not affect the accuracy considerably while decreasing it made it hard to gauge the complete performance of the ML models on testing data. We need around a minimum of 10-50 pulses in the testing dataset to measure the slight variations that may arise in predicting the clear pulsar profiles. During testing, we give the model the values of X_{test} (raw profiles), and the models predict the values of y_{test} variable, which represents the denoised profiles. The testing dataset forms 16.67% of the total dataset of a pulsar in all the pulsars tested and for all the algorithms used in this work.

2.5. Feature Scaling

Feature scaling is a process in which the features or independent variables of the data are normalized to constrain them in a specific range. Sometimes, since the raw data range varies widely, in some machine learning models, the loss calculation functions would not yield satisfactory results without normalizing the features. For example, many algorithms utilize the Euclidean distance between multiple points to calculate the loss function, and if one of the features consists of a broad range of values, this feature will overpower other features when the model learns the data, and it will become biased towards that particular feature. To eliminate this issue, Feature scaling is implemented [27] [28]. Since we have a broadly varied raw data, this technique has been incorporated in this work. Feature scaling has many different types, but we have used the most simple Min-Max Normalization technique which performs a comprehensive rescale of the input data into a range of [0,1] or [-1,1]. Since the total pulsar intensity can never be negative, We have rescaled the data into an output range of [0,1]. The general formula for Min-Max Normalization is:-

$$x' = \frac{x - \min(x)}{\max(x) - \min(x)} \quad (2)$$

where x is the original value and x' is the normalized value of the input feature, and $\max(x)$, $\min(x)$ denote the maximum and the minimum values of x respectively.

3. Models deployed

We have tested 7 different machine learning algorithms for the pulsars selected. All these algorithms have been implemented using the scikit-learn library [29] in Python 3.6 programming language. The subclass `sklearn.ensemble` provides a number of machine learning ensemble (section-3.3) techniques like Adaboost, Random forest, Gradient boosting, and others.

3.1. Linear Regression

Linear regression defines a simple relationship between one or more independent variables and a dependent variable through a straight line. These relationships are modelled using linear predictor functions whose model parameters are estimated from the data. Once we know the values of the predictors, linear regression calculates the conditional probability distribution, instead of using the joint probability distribution of all of those variables, which lies in the expertise of Multivariate analysis [30] [31].

In the case of prediction, error minimization and forecasting, Linear Regression models have been used rigorously. These are limited by the linear relationship between input and output variables, but they work very well for simple cases. Mathematically the objective function to be minimized in case of Linear regression is given by the following:-

$$Z = \text{MIN} \sum_{i=1}^n (y_i - w_i x_i)^2 \quad (3)$$

where y_i is the output variable, w_i is the coefficient of x , and x_i is the input feature under study. MIN denotes that the regression tries to minimize the objective function by finding a suitable value of w_i . This method is also termed as Ordinary Least Squares (OLS). A comparison of the predictions of this model with the testing dataset is plotted in figure-A1

3.2. Decision Tree Regressor

A Decision tree is a part of Decision Tree Learning which uses a decision tree (as a predictive model) to go from observations about an item (represented in the branches) to conclusions about the item's target value (represented by the leaves) [32] [33]. There are two basic types of trees– Classification tree:- In these trees, leaves represent class labels and branches represent the combinations of features that lead to those class labels. Regression Trees:- In these trees, the target variable is not restricted to any particular class but can take any real value. It is this type of decision tree that we are going to use as a predictive model. A decision tree can be used to visually and explicitly represent many types of decision-making scenarios.

A sample input data comes in the form $(x, Y) = (x_1, x_2, x_3, \dots, x_n, Y)$ where x_1, x_2, x_3, \dots are the inputs and Y is the output. In all the pulsars we have used, and for all the algorithms tested, there is only one input variable, the array of the raw data, and one output to be predicted, i.e., the array which contains the profile after denoising. A comparison of the predictions of this model with the testing dataset is plotted in figure-A1

3.3. Ensemble Methods

In Machine Learning and Statistics, many different algorithms are utilized in Ensemble methods, rather than a single algorithm to get better predictive performance than that can be possibly achieved by any single algorithm alone [34] [35]. A machine learning ensemble is different from a statistical ensemble technique in the sense that it consists of only a finite discrete number of alternative algorithms rather than an infinite number in Statistical Mechanics. Ensemble learning models are strong candidates for our approach, extensively used to search and identify pulsar classes. Ensemble candidate classification has been deployed for LOTAAS pulsar survey [36], FAST drift-scan survey [37], and [38] where Random forest, an ensemble learning-based approach has been used for pulsar search. These works have inspired us to use an ensemble learning approach majorly for our analysis where we have deployed the following ML ensemble models:-

3.3.1. Gradient Boosting Regressor

Boosting in machine learning is the process of transformation of a weak learner (an algorithm just classifying or predicting values better than a random guess) into a strong learner (an algorithm, which is arbitrarily well correlated with the true output data). It originated when renowned American Computer Scientist Robert Schapire answered [39] a famous question put up by Michael Kearns and Leslie Valiant in 1988 and 1989 [40] [41]. Boosting involves incrementally constructing an ensemble by training each new model instance to highlight those training instances that previous models misclassified. A framework governs the eligibility of an algorithm to be a boosting algorithm; this framework is called as Probably Approximately Correct (PAC) learning formulation. Only those algorithms that are provable in this formulation can be characterized as boosting algorithms.

Gradient boosting is a machine learning technique for classification and regression problems. An ensemble of weak prediction models (in the form of decision trees) constitutes a new prediction model [42]. Gradient boosting constructs the model in a stage-wise fashion that other boosting methods [boosting methods] do, and the decision trees are generalized by allowing optimization of an arbitrary differentiable loss function, which is also called gradient descent. A comparison of the predictions of this model with the testing dataset is plotted in figure-A1

3.3.2. Adaboost Regressor

Adaboost is the most popular boosting algorithm and the most significant in Ensemble learning history as it could adapt to weak learners before any other boosting algorithm could do it. This technique

can be used both for classification as well as regression [43] [44]. Decision trees having a single split, called Decision stumps, constitute the weak learners in Adaboost. After training a regressor at any level, Adaboost assigns weight to each training item. Higher weight is assigned to a wrongly predicted item so that the next regressor's (with higher probability) training subset includes that item in it. Once the training of each regressor is complete, the regressor is assigned a weight based on its accuracy. Those regressors having higher accuracy are assigned greater weights to improve their impact on the final outcome. A regressor with 50% accuracy is offered a zero weight, and a regressor with less than 50% accuracy is offered a negative weight. A comparison of the predictions of this model with the testing dataset is plotted in figure-A1

3.3.3. Random Forest Regressor

Random forests are an ensemble learning approach for regression, classification and other tasks that function by building a plethora of decision trees at the time of training and presenting a class that is the mode of the classes considered (classification) or the mean prediction (regression) of individual trees [45] [46]. Decision trees are sometimes guilty of overfitting to the training data, and Random forest corrects this habit of decision trees. In our problem, we are going to use the Random Forest algorithm for regression purposes. A comparison of the predictions of this model with the testing dataset is plotted in figure-A1

3.4. K Nearest Neighbours

In the machine learning world, K Nearest Neighbours is a non-parametric method proposed by Thomas Cover [47] which is used for both classification and regression [48]. The KNN model's output depends upon the operation to be performed; for classification purpose, the model predicts the parent class of a new data point. For regression purposes, the model predicts a real value called the property value of the new data point. The model's input is the nearest N neighbouring data points by considering the Euclidean distance between the new data point and its N nearest neighbours. The following equation gives the Euclidean distance for any two arbitrary points p and q:-

$$d(p, q) = d(q, p) = \sqrt{(q_1 - p_1)^2 + (q_2 - p_2)^2 + \dots + (q_n - p_n)^2} = \sqrt{\sum_{i=1}^n (q_i - p_i)^2} \quad (4)$$

Here, n denotes the dimensions of the point (n=2 for 2D space and n=3 for 3D space). For all the pulsars tested, values of K were decided from hyperparameter optimization [49]. A comparison of the predictions of this model with the testing dataset is plotted in figure-A1

3.5. Support Vector Regressor (SVR)

Unlike in OLS (Eqn-3), SVR enables the user to specify the error bar, i.e., it constructs a line or a hyperplane (in higher dimensions) to account for the desired level of acceptance of the errors obtained. That essentially implies that the model does not care how large are the errors, provided they lie within a particular pre-specified error bar [50] [51]. A comparison of the predictions of this model with the testing dataset is plotted in figure-A1

4. Results

We now present the results of the various machine learning algorithms used to denoise our pulsar signals. 4 Model evaluation parameters have been used for this purpose:-

- R2 score:- This is an important parameter used very commonly in the machine learning field. It characterises the deviation in the target variable, which can be correctly explained by the independent variables. In other words, this parameter evinces the goodness of fit of an ML model.
- Mean Absolute Error (MAE):- Statistically, Mean Absolute Error(MAE) refers to the mean of the absolute values of each prediction error on every instance of the test dataset. The prediction error is the difference between the actual value and predicted value at that instance. [to be refined and cited]. The following formulation can represent it:-

$$MAE = \frac{\sum_{i=1}^n abs(y_i - \gamma(x_i))}{n} \quad (5)$$

where y_i denotes the real output, and $\gamma(x_i)$ denotes the predicted value by the ML model.

- Mean Squared Error (MSE):- It is the sum, over all the data points, of the square of the difference between the predicted and actual target variables, divided by the number of data points. Due to the nature of this error's squared dependence, it penalizes the bigger errors more severely. It is calculated by the following formula:-

$$MSE = \frac{\sum_{i=1}^n (y_i - \gamma(x_i))^2}{n} \quad (6)$$

- Root Mean Squared Error (RMSE) :- RMSE is the square root of MSE. MSE is measured in units that are the square of the target variable, while RMSE is measured in the same units as the target variable. It is calculated by :-

$$RMSE = \sqrt{\frac{\sum_{i=1}^n (y_i - \gamma(x_i))^2}{n}} \quad (7)$$

4.1. Result Plots

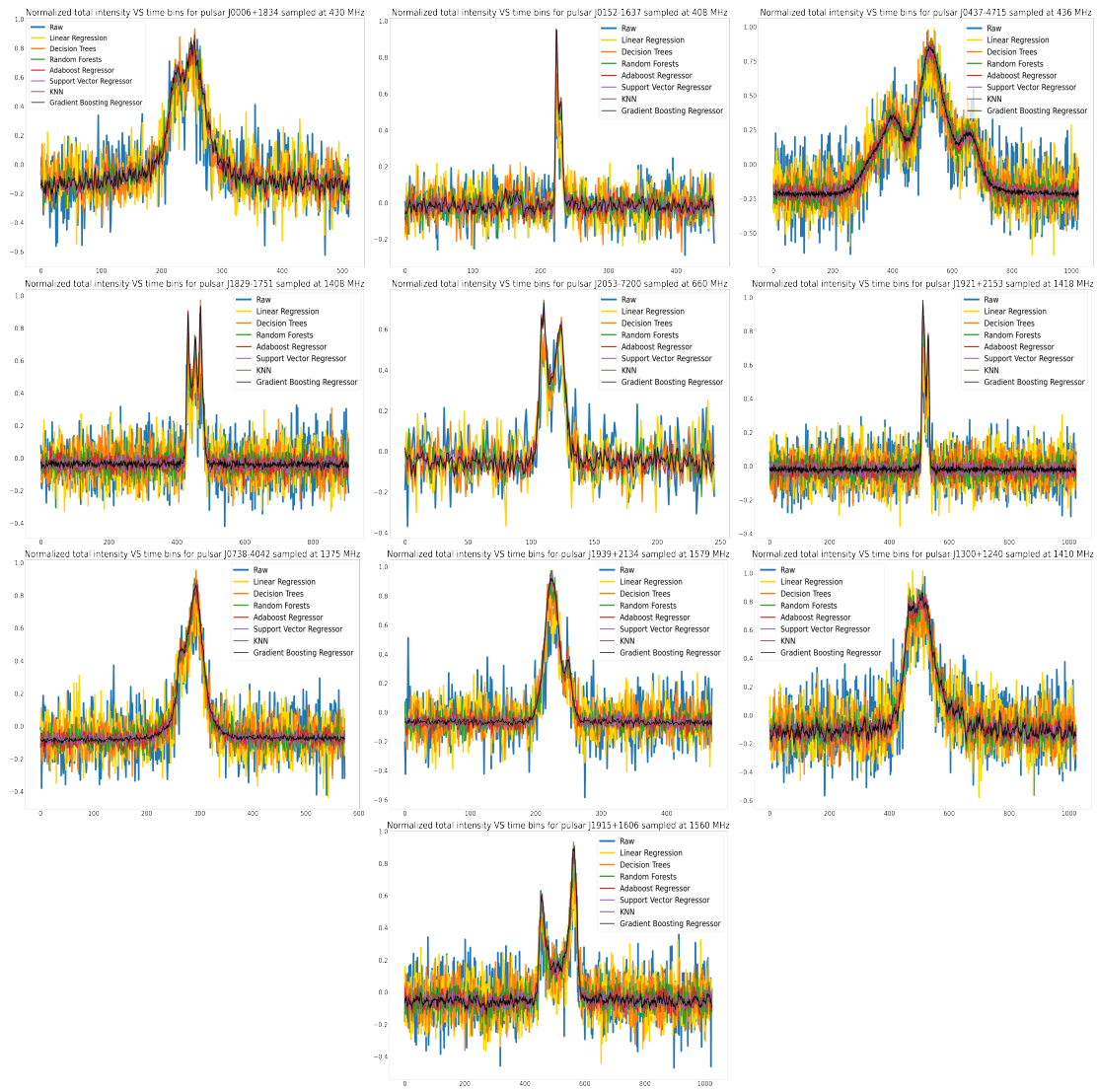


Figure 2. Raw Profiles and denoised profiles as predicted by different algorithms for different pulsars.

4.2. Linear Regression

As it is evident from the graphs obtained (fig-2), the Linear regression model shows an average R2 score of 86.78% for training and 86.03% for testing (table-2 and table-3) which is not that high as that achieved by other algorithms as we will explore more of them. Linear regression is not able to produce a good fit due to its primitiveness which was expected too. The average MAE, MSE and RMSE are the highest of all the algorithms tested. The obtained profile still consists of a significant amount of noise, which is clear from the average SNR of 5.93 obtained for the output profiles.

4.3. Decision Tree Regressor

Decision tree regression shows an exceptional average R2 score of 98.95% for training and a slightly better testing R2 score than Linear regression at 87.3%, which means that the model has learned the

training data too well, but has performed quite poorly for testing data, showing clear signs of overfitting. One of the reasons could be that the training dataset was more than that was required. MAE, MSE and RMSE are lower too. The SNRs obtained for the output profiles were slightly higher at 7.07.

4.4. Random Forest Regressor

While looking at the results for Random forest regressor having the average R2 scores of 98.53% for training and 90.48% for testing and slightly lower MAE, MSE and RMSE, it is observed that while performing better than Decision tree regressor, the overfitting problem has been reduced but not completely eradicated, and hence better algorithms are required. An improvement of 19.57% was obtained in the output SNR over Decision tree regressor.

4.5. Adaboost Regressor

Adaboost regressor shows an ameliorated response, with the average R2 scores 92.63% for training and 90.52% for testing with lower MAE, MSE and RMSE. It has finally solved the overfitting problem that the Decision tree and random forest regressors suffered with.

4.6. Support Vector Regressor

Support vector regressor shows an impressive result, with an average R2 score of 93.45% for training and 93.3% for testing, and lower MAE, MSE and RMSE too than all of the above algorithms tested. SVR shows the first significant improvement in the SNRs obtained. The average SNRs obtained for the output profiles is 21.31, which is a big jump from the initial SNR of 4.23 (raw profile).

4.7. KNN Regressor

With R2 scores of 94.35% for training and 93.48% for testing, KNN has performed better than SVR and significantly better than the first three algorithms. MAE, MSE and RMSE are the lowest of all the above algorithms and the average output SNR obtained is 29.32, which is again an impressive boost from the raw profile.

4.8. Gradient Boosting Regressor

After analysing the results for Gradient boosting regressor (table-2 and table-3), it can be concluded that it performs similar to the KNN regressor, with very close R2 scores of 94.52% for training and 94.4% for testing. MAE, MSE and RMSE are also similar to that obtained by KNN. It also performs the best with the average output SNR of 30.63.

Table 2. Input and output SNRs obtained for different algorithms

Algorithms tested	Average SNR of pulsar profiles	
	Before denoising	After denoising
Linear Regression	4.23	5.93
Decision Tree Regressor	4.23	7.07
Random Forest Regressor	4.23	7.75
Adaboost Regressor	4.23	11.55
Support Vector Regressor	4.23	21.31
KNN Regressor	4.23	29.32
Gradient Boosting Regressor	4.23	30.63

Table 3. Performance parameter scores of different ML models on different pulsars tested

ML Models	Performance parameters			
	R2 Score (train,test %)	MAE	MSE	RMSE
Linear Regression	(86.78,86.03)	0.06522	0.007915	0.08896
Decision Tree Regressor	(98.95, 87.3)	0.06302	0.007589	0.08710
Random Forest Regressor	(98.53,90.48)	0.05941	0.005886	0.07672
Adaboost Regressor	(92.63,90.52)	0.05713	0.005460	0.07389
Support Vector Regressor	(93.45,93.3)	0.05325	0.005133	0.07164
KNN Regressor	(94.35,93.48)	0.048720	0.004685	0.06844
Gradient Boosting Regressor	(94.52,94.4)	0.04512	0.004478	0.06691

Finally, we demonstrate the pulsar SNR variation for different pulsars after SNR improvement by the best performing algorithm, Gradient boosting regressor. The results are summarised in table-4. Graph of pulsar SNR for J1300+1240 with the number of folding periods for a pulsar photon signal is shown in fig-3. Point to be noted is that all the pulsars showed similar nature of the graph.

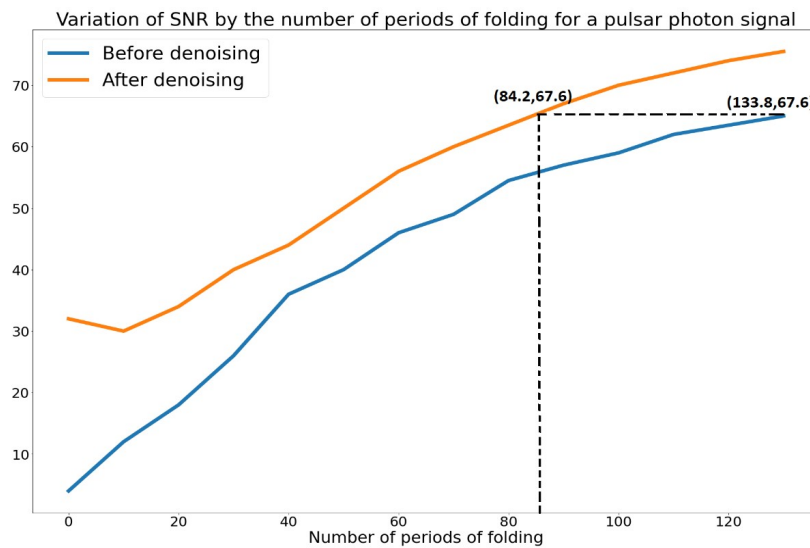


Figure 3. Variation of SNR with period for pulsar J1300+1240 by Gradient Boosting regressor. The raw profile(profile before denoising) is shown in blue color and the denoised profile is shown in orange color.

Table 4. Demonstration of efficiency of this approach for the pulsars tested

Pulsars	Initial SNR before folding		Periods to reach SNR of 67.6	
	Raw profile	denoised profile by GBR	before denoising	after denoising
J0006+1834	4.15	30.56	134.2	84.3
J0152-1637	4.2	27.33	139.4	88.1
J0437-4715	4.32	34.85	125.3	81.2
J1829-1751	4.53	31.32	133.4	85.7
J2053-7200	4.10	25.10	142.2	89.2
J2145-0750	4.22	35.32	125.1	81.3
J1300+1240	4.02	29.35	136.5	86.3
J1915+1606	4.17	32.10	133.1	84.6
J0738-4042	4.23	31.05	134.3	84.2
J0250+5854	4.31	29.37	136.4	86.1

As evident from the figure, the augmented SNR of the pulsar by the Gradient boosting regressor is greater than the raw data, at every epoch of folding. The initial SNRs at 0 folding are 4 and 32.5 respectively for raw and the filtered profiles. A major point here is to be noted that while the unfiltered profile takes more than 133 periods of folding to achieve an SNR of 67.6, the filtered profile takes only 84 periods, which means that lower periods of observation will be required by the telescopes which will improve their overall performance effectively. The rate of SNR increase vs the number of folding periods for both the profiles keeps decreasing continuously, giving us a picture that they may saturate over very high periods of folding. Testing with other pulsars showed similar results.

5. Discussion and Conclusion

The results that are obtained here pave the way towards greater inclusion of machine learning algorithms in the pulsar denoising field, especially since the testing process for the ML algorithms takes a negligible amount of time to produce denoised profiles, from the Gaussian noise, which could be sent to folding algorithms to improve the SNRs even further. In future work, an effort will be made to apply these algorithms for pulsar data embedded in real noise with much lower initial SNRs to see if they are equally effective in improving the SNRs just as they are for pulsar data with Gaussian noise. Suppose we already have pulsars with high SNRs before sending those profiles to the folding algorithm. In that case, it is imperative that a lesser number of periods would be required for pulsar folding, which also implies that the telescope would need to observe the pulsars for a shorter duration of time to generate the same SNR after folding, and thus, we can generate high-quality single pulse profiles using a combination of Machine Learning and Folding techniques in a more effective manner. Some head-start has already been made in this, where deep Recurrent neural networks have been used to denoise the pulsar profiles [13], but the initial SNR which was sent to the RNN algorithm was hovering around 6 in their work which is on the higher side as compared to our work.

Acknowledgments: We are very thankful to Dr. Arunima Banerjee, Assisant Professor, Indian Institute of Science Education and Research (IISER) Tirupati, India, for her guidance and ideas regarding this work. We are also thankful to Mr. Ankul Prajapati, Pierre and Marie Curie Campus, Sorbonne University, Paris, France for his constant support and vital suggestions towards the improvement of our work. Part of this research has made use of the EPN Database of Pulsar Profiles maintained by the University of Manchester, available at: <http://www.jodrellbank.manchester.ac.uk/research/pulsar/Resources/epn/w>

References

1. Myers, J. Imagine the Universe ! https://imagine.gsfc.nasa.gov/science/objects/neutron_stars1.html, accessed on 12.09.2020.
2. Robertson, P. An Australian Icon-Planning and Construction of the Parkes Telescope. *arXiv preprint arXiv:1210.0987* **2012**.
3. team, C. About Parkes radio telescope. <https://www.csiro.au/en/Research/Facilities/ATNF/Parkes-radio-telescope/About-Parkes>, accessed on 12.09.2020.
4. Swarup, G. Giant Metrewave Radio Telescope—Its possible use for SETI. *Acta Astronautica* **1992**, *26*, 239–242.
5. Atwood, W.; Abdo, A.A.; Ackermann, M.; Althouse, W.; Anderson, B.; Axelsson, M.; Baldini, L.; Ballet, J.; Band, D.; Barbiellini, G.; others. The large area telescope on the Fermi gamma-ray space telescope mission. *The Astrophysical Journal* **2009**, *697*, 1071.
6. Hotan, A.; Van Straten, W.; Manchester, R. PSRCHIVE and PSRFITS: an open approach to radio pulsar data storage and analysis. *Publications of the Astronomical Society of Australia* **2004**, *21*, 302–309.
7. van Straten, W.; Bailes, M. DSPSR: digital signal processing software for pulsar astronomy. *Publications of the Astronomical Society of Australia* **2011**, *28*, 1–14.
8. Price, D.; Staveley-Smith, L.; Bailes, M.; Carretti, E.; Jameson, A.; Jones, M.; van Straten, W.; Schediwy, S. HIPSR: A digital signal processor for the Parkes 21-cm Multibeam Receiver. *Journal of Astronomical Instrumentation* **2016**, *5*, 1641007.
9. Susobhanan, A.; Maan, Y.; Joshi, B.C.; Prabu, T.; Desai, S.; Gupta, Y.; Gopakumar, A.; Batra, N.D.; Choudhary, A.; Surnis, M.P.; others. pinta: The uGMRT Data Processing Pipeline for the Indian Pulsar Timing Array. *arXiv preprint arXiv:2007.02930* **2020**.
10. Devine, T.R.; Goseva-Popstojanova, K.; McLaughlin, M. Detection of dispersed radio pulses: a machine learning approach to candidate identification and classification. *Monthly Notices of the Royal Astronomical Society* **2016**, *459*, 1519–1532.
11. Morello, V.; Barr, E.; Bailes, M.; Flynn, C.; Keane, E.; van Straten, W. SPINN: a straightforward machine learning solution to the pulsar candidate selection problem. *Monthly Notices of the Royal Astronomical Society* **2014**, *443*, 1651–1662.
12. Florez, A.Y.C.; Vinces, B.V.S.; Arroyo, D.C.R.; Saire, J.E.C.; Franco, P.B. Machine Learning Pipeline for Pulsar Star Dataset. *arXiv preprint arXiv:2005.01208* **2020**.
13. Jiang, Y.; Jin, J.; Yu, Y.; Hu, S.; Wang, L.; Zhao, H. Denoising Method of Pulsar Photon Signal Based on Recurrent Neural Network. *2019 IEEE International Conference on Unmanned Systems (ICUS)* **2019**, pp. 661–665.
14. Bethapudi, S.; Desai, S. Separation of pulsar signals from noise using supervised machine learning algorithms. *Astronomy and Computing* **2018**, *23*, 15–26. doi:10.1016/j.ascom.2018.02.002.
15. Zhang, C.J.; Shang, Z.H.; Chen, W.M.; Xie, L.; Miao, X.H. A Review of Research on Pulsar Candidate Recognition Based on Machine Learning. *Procedia Computer Science* **2020**, *166*, 534–538.
16. McFadden, R.; Karastergiou, A.; Roberts, S. Machine learning for pulsar detection. *Proceedings of the International Astronomical Union* **2017**, *13*, 372–373.
17. Keith, M. The EPN Database of Pulsar Profiles. <http://www.epta.eu.org/epndb/>, accessed on 12.09.2020.
18. Lorimer, D.; Jessner, A.; Seiradakis, J.; Lyne, A.; D’Amico, N.; Athanasopoulos, A.; Xilouris, K.; Kramer, M.; Wielebinski, R. A flexible format for exchanging pulsar data. *Astronomy and Astrophysics Supplement Series* **1998**, *128*, 541–544.
19. Backer, D.C.; Kulkarni, S.R.; Heiles, C.; Davis, M.; Goss, W. A millisecond pulsar. *Nature* **1982**, *300*, 615–618.
20. database maintaining team, A. ANTF Pulsar Catalogue. <https://www.atnf.csiro.au/research/pulsar/psrcat/>, accessed on 12.09.2020.
21. Hessels, J.W.; Ransom, S.M.; Stairs, I.H.; Freire, P.C.; Kaspi, V.M.; Camilo, F. A radio pulsar spinning at 716 Hz. *Science* **2006**, *311*, 1901–1904.
22. Pavlov, G.G.; Kargaltsev, O.; Garmire, G.; Wolszczan, A. X-ray emission from the planet pulsar B1257+ 12. *The Astrophysical Journal* **2007**, *664*, 1072.

23. Hobbs, G.; Faulkner, A.; Stairs, I.; Camilo, F.; Manchester, R.; Lyne, A.; Kramer, M.; D'Amico, N.; Kaspi, V.; Possenti, A.; others. The Parkes multibeam pulsar survey–IV. Discovery of 180 pulsars and parameters for 281 previously known pulsars. *Monthly Notices of the Royal Astronomical Society* **2004**, 352, 1439–1472.
24. Brook, P.; Karastergiou, A.; Buchner, S.; Roberts, S.; Keith, M.; Johnston, S.; Shannon, R. Evidence of an asteroid encountering a pulsar. *The Astrophysical Journal Letters* **2013**, 780, L31.
25. Tan, C.; Bassa, C.; Cooper, S.; Dijkema, T.; Esposito, P.; Hessels, J.; Kondratiev, V.; Kramer, M.; Michilli, D.; Sanidas, S.; others. Lofar discovery of a 23.5-second radio pulsar. *arXiv preprint arXiv:1809.00965* **2018**.
26. Ying, X. An overview of Overfitting and its solutions. *Journal of Physics: Conference Series*. IOP Publishing, 2019, Vol. 1168, p. 022022.
27. Raschka, S. About feature scaling and normalization and the effect of standardization for machine learning algorithms. *Polar Political Legal Anthropology Rev* **2014**, 30, 67–89.
28. Singh, D.; Singh, B. Investigating the impact of data normalization on classification performance. *Applied Soft Computing* **2019**, p. 105524.
29. Pedregosa, F.; Varoquaux, G.; Gramfort, A.; Michel, V.; Thirion, B.; Grisel, O.; Blondel, M.; Prettenhofer, P.; Weiss, R.; Dubourg, V.; others. Scikit-learn: Machine learning in Python. *the Journal of machine Learning research* **2011**, 12, 2825–2830.
30. Rong, S.; Bao-wen, Z. The research of regression model in machine learning field. *MATEC Web of Conferences*. EDP Sciences, 2018, Vol. 176, p. 01033.
31. Strehl, A.L.; Littman, M.L. Online linear regression and its application to model-based reinforcement learning. *Advances in Neural Information Processing Systems*, 2008, pp. 1417–1424.
32. Navada, A.; Ansari, A.N.; Patil, S.; Sonkamble, B.A. Overview of use of decision tree algorithms in machine learning. 2011 IEEE control and system graduate research colloquium. IEEE, 2011, pp. 37–42.
33. Loh, W.Y. Classification and regression trees. *Wiley Interdisciplinary Reviews: Data Mining and Knowledge Discovery* **2011**, 1, 14–23.
34. Dietterich, T.G. Ensemble methods in machine learning. *International workshop on multiple classifier systems*. Springer, 2000, pp. 1–15.
35. Zhou, Z.H. Ensemble Learning. *Encyclopedia of biometrics* **2009**, 1, 270–273.
36. Tan, C.M.; Lyon, R.; Stappers, B.; Cooper, S.; Hessels, J.; Kondratiev, V.; Michilli, D.; Sanidas, S. Ensemble candidate classification for the LOTAAS pulsar survey. *Monthly Notices of the Royal Astronomical Society* **2018**, 474, 4571–4583.
37. Wang, H.; Zhu, W.; Guo, P.; Li, D.; Feng, S.; Yin, Q.; Miao, C.; Tao, Z.; Pan, Z.; Wang, P.; others. Pulsar candidate selection using ensemble networks for FAST drift-scan survey. *SCIENCE CHINA Physics, Mechanics & Astronomy* **2019**, 62, 959507.
38. Azhari, M.; Alaoui, A.; Abarda, A.; Ettaki, B.; Zerouaoui, J. A Comparison of Random Forest Methods for Solving the Problem of Pulsar Search. *The Proceedings of the Third International Conference on Smart City Applications*. Springer, 2019, pp. 796–807.
39. Schapire, R.E. The strength of weak learnability. *Machine learning* **1990**, 5, 197–227.
40. Kearns, M. Thoughts on hypothesis boosting. *Unpublished manuscript* **1988**, 45, 105.
41. Kearns, M.; Valiant, L. Cryptographic limitations on learning Boolean formulae and finite automata. *Journal of the ACM (JACM)* **1994**, 41, 67–95.
42. Natekin, A.; Knoll, A. Gradient boosting machines, a tutorial. *Frontiers in neurorobotics* **2013**, 7, 21.
43. Schapire, R.E. Explaining adaboost. In *Empirical inference*; Springer, 2013; pp. 37–52.
44. Solomatine, D.P.; Shrestha, D.L. AdaBoost. RT: a boosting algorithm for regression problems. 2004 IEEE International Joint Conference on Neural Networks (IEEE Cat. No. 04CH37541). IEEE, 2004, Vol. 2, pp. 1163–1168.
45. Liaw, A.; Wiener, M.; others. Classification and regression by randomForest. *R news* **2002**, 2, 18–22.
46. Biau, G.; Scornet, E. A random forest guided tour. *Test* **2016**, 25, 197–227.

47. Chomboon, K.; Chujai, P.; Teerarassamee, P.; Kerdprasop, K.; Kerdprasop, N. An empirical study of distance metrics for k-nearest neighbor algorithm. *Proceedings of the 3rd international conference on industrial application engineering*, 2015, pp. 280–285.
48. Burba, F.; Ferraty, F.; Vieu, P. k-Nearest Neighbour method in functional nonparametric regression. *Journal of Nonparametric Statistics* **2009**, *21*, 453–469.
49. Fraj, M.B. In Depth: Parameter tuning for KNN. <https://medium.com/@mohtedibf/in-depth-parameter-tuning-for-knn-4c0de485baf6>, accessed on 12.09.2020.
50. Drucker, H.; Burges, C.J.; Kaufman, L.; Smola, A.J.; Vapnik, V. Support vector regression machines. *Advances in neural information processing systems*, 1997, pp. 155–161.
51. Awad, M.; Khanna, R. Support vector regression. In *Efficient learning machines*; Springer, 2015; pp. 67–80.

Appendix A Additional Details

The following images demonstrate the Predicted profiles vs testing data fit showing us how the different machine learning models interpreted the testing data and made predictions:-

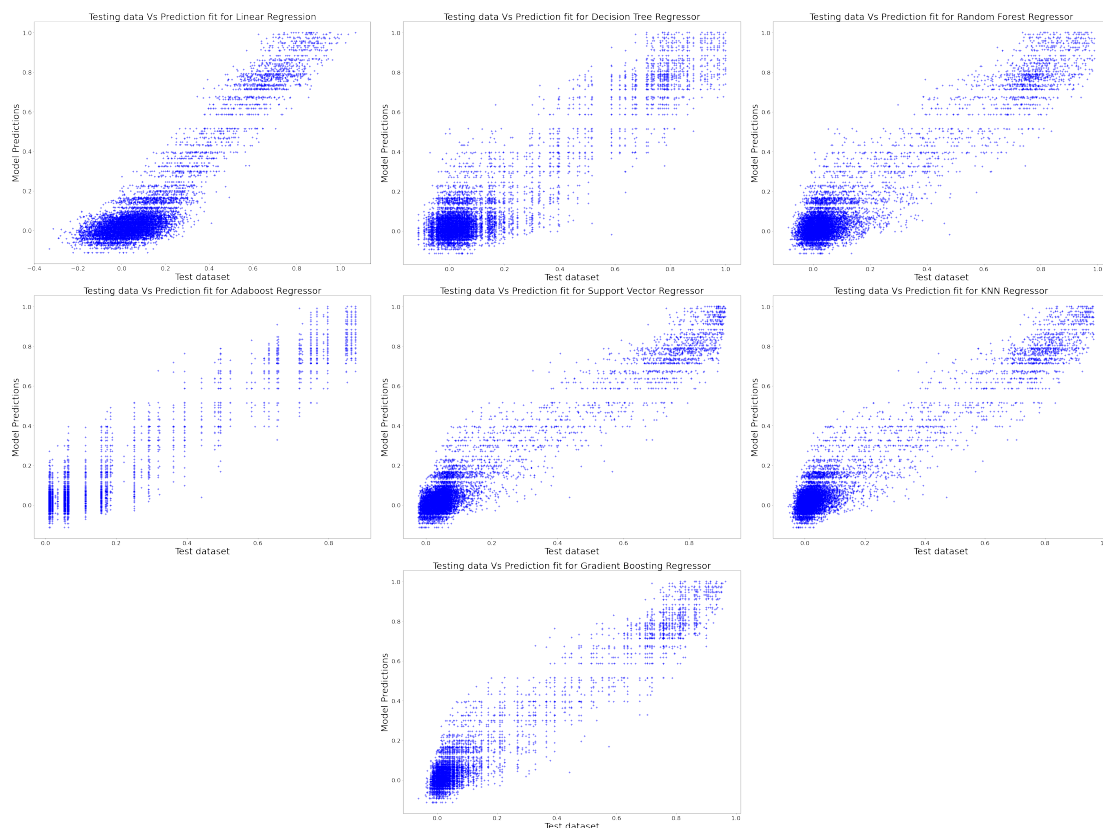


Figure A1. Figures show the predicted data values by different models as compared to that of the testing data for pulsar J0006+1834